

Universal quantum control with error correction

Zhu-yao Jin¹ and Jun Jing^{1,*}

¹*School of Physics, Zhejiang University, Hangzhou 310027, Zhejiang, China*

(Dated: February 28, 2025)

Error correction is generally demanded in large-scale quantum information processing and quantum computation. We here provide a universal and realtime control strategy to cope with arbitrary type of errors in the system Hamiltonian. The strategy provides multiple error-resilient paths of the interested system by the von Neumann equation for ancillary projection operators. With no extra control fields and precise designs, only the path-dependent global phase is required to vary rapidly to suppress the error-induced transitions among distinct paths. Those corrected paths can also be regarded as the approximate solutions to the time-dependent Schrödinger equation perturbed by errors. We practice the strategy with the cyclic transfer of populations in a three-level system, showing a superior error-resilience to parallel transport. Our universal control theory can advance the performance of various quantum tasks on imperfect systems.

I. INTRODUCTION

Quantum computer has extra advantages over its classical counterpart in solving certain problems [1, 2], e.g., the Shor's algorithm for factoring large numbers [3, 4]. However, factoring a 2048-bit RSA integer demands 20 millions of physical qubits and 2.7 billions of Toffoli-gate with error rates of 10^{-10} per gate [5]. In sharp contrast, the state-of-the-art quantum processors typically exhibit error rates of 10^{-3} per gate [6–9], which remain far too high for the execution of a practical circuit. Without a fault-tolerant design, quantum computation would be restricted to problems so small that they would be of little use or interest. With quantum error correction (QEC) [10], it is strongly believed to be scaled up to a reasonably large size towards the powerful calculation of tomorrow. The key to QEC is to identify the error resources and then to compensate for their effect.

In the first QEC scheme [10], 9 physical qubits are used to encode one logical qubit to address the errors caused by environmental decoherence. Due to the redundancy of a large Hilbert space, the failure of any physical qubit does not corrupt the underlying logical information and can be unambiguously detected and corrected in real time [11]. Inspired by the Shor's code, many QEC coding schemes [12–21] have been proposed, including Bacon-Shor [12], color [13], five-qubit [14], heavy-hexagon [15], surface [16, 17], and continuous-variable codes [18–21]. Their usefulness can be assessed by the so-called break-even point [22–24]. In other words, the lifetime of the encoded logical qubits should be larger than that of the best available physical qubits. The excess over the break-even point was firstly demonstrated in the superconducting qubit system [22], followed by the quantum electrodynamics architecture [23] and the trapped-ion system [24].

Another main error source is the system fluctuation, which typically arises from imperfect knowledge of the system or variations in the experimental param-

eters during practical implementation. As an early approach in nuclear magnetic resonance [25], the composite-pulse method [26–37] utilizes multiple pulses with well-designed shapes to compensate for the systematic errors in such as the time duration [28, 30, 33], the detuning [34, 35], and the phase [27, 29, 32]. To avoid the high-resource cost associated with multiple pulses, the single-shot pulse method [38–40] based on perturbation theory is proposed to locate and compensate for the systematic errors through adjusting the global phase. This method can be interpreted in terms of geometry [41–43] in Hilbert space. As a general dynamical-decoupling method, non-perturbative leakage elimination operators [44] were introduced to neutralize the errors with a sufficient large integral of the pulse sequence within the time domain. In addition, the degree of tolerance against systematic errors can be enhanced by nonadiabatic controls, including the digital optimization method [45], the numerical optimization algorithm [46], the dark-path schemes [47–49], the measurement-based mitigation method [50], and the pulse-shaping method [51]. Most of them focused on the systems of a few levels and with the $SU(2)$ dynamic symmetry [52] and their applicability is restricted to certain type of errors. A universal control framework applicable to discrete systems of any dimension and resilient to arbitrary systematic error is apparently desired.

In this paper, we develop a forward-engineering framework for active-controlling the system dynamics perturbed by arbitrary type of systematic errors. The system dynamics is prescribed in an ancillary picture spanned by the nonadiabatic paths that can be determined by the von Neumann equation for the ancillary projection operators. In the absence of systematic errors, no transition occurs among the nonadiabatic paths during the time evolution. In the nonideal situations, the errors can be identified in the second-rotated picture by using the Magnus expansion. The global phase of a desired path is found to be a crucial degree of freedom to suppress the unwanted transitions to the other paths, irrespective of the error type. It has not yet been discussed in conventional control methods, such as shortcuts to adiabaticity [53–58] and the nonadiabatic holonomic transformation [51, 59]

* Email address: jingjun@zju.edu.cn

under the parallel-transport condition [60, 61]. We illustrate our theory with the cyclic transfer of populations in an ubiquitous three-level system.

The rest part of this paper is structured as follows. In Sec. II A, we recall our general control framework that demonstrates multiple nonadiabatic paths under an error-free time-dependent Hamiltonian. In Sec. II B, it is extended to the nonideal situation perturbed by a general error Hamiltonian. Arbitrary type of systematic errors are identified within a second-rotated picture and then be suppressed to the second order of error magnitude. By rapidly manipulating the path-dependent global phase, as a practical correction mechanism, we show the error-resilience of our control theory in the presence of either commutative or noncommutative errors in Sec. III. Section IV examines our correction control subject to these two types of errors during the cyclic transfer of populations of a general three-level system. The whole work is concluded in Sec. V. Appendix A provides a detailed construction of universal passages for a non-degenerate three-level system in the absence of errors.

II. GENERAL FRAMEWORK

In this section, the open-quantum-system control with error correction is performed under our universal framework [62] proposed to unify the the transitionless dynamics [63], the shortcuts to adiabaticity [53–56, 58], the holonomic quantum transformation [51, 59], and the reverse engineering method [39, 41, 64, 65]. It was developed on the idea as a quantum generalization of the d’Alembert’s principle about the virtual displacement. We first briefly review the general framework with an error-free Hamiltonian and then extend it to the nonideal situations with systematic errors.

A. Ideal situation

The universal perspective on nonadiabatic quantum control [62] is firstly conducted on a closed quantum system of arbitrary finite size driven by a well-defined and time-dependent Hamiltonian $H_0(t)$. The system dynamics is given by the time-dependent Schrödinger equation as ($\hbar \equiv 1$)

$$i \frac{d|\psi_m(t)\rangle}{dt} = H_0(t)|\psi_m(t)\rangle, \quad (1)$$

where $|\psi_m(t)\rangle$ ’s are the pure-state solutions. Suppose the Hilbert space of the system is K dimensional then m runs from 1 to K when $H_0(t)$ is full rank. The time-evolution operator $U_0(t)$ about $H_0(t)$ is generally hard to be found unless $|\psi_m(t)\rangle$ ’s have already constituted an orthonormal set for the Hilbert space of the system.

Alternatively, the time-dependent Schrödinger equation (1) can be treated within a rotated picture spanned by the ancillary basis states $|\mu_k(t)\rangle$ ’s, $1 \leq k \leq K$, that

span the same Hilbert space as $|\psi_m(t)\rangle$ ’s. In the rotating frame with respect to $V(t) \equiv \sum_{k=1}^K |\mu_k(t)\rangle \langle \mu_k(0)|$, Eq. (1) is transformed to be

$$i \frac{d|\psi_m(t)\rangle_{\text{rot}}}{dt} = H_{\text{rot}}(t)|\psi_m(t)\rangle_{\text{rot}}, \quad (2)$$

where the rotated pure-state solutions $|\psi_m(t)\rangle_{\text{rot}}$ are written as

$$|\psi_m(t)\rangle_{\text{rot}} = V^\dagger(t)|\psi_m(t)\rangle, \quad (3)$$

and the rotated system Hamiltonian $H_{\text{rot}}(t)$ reads

$$\begin{aligned} H_{\text{rot}}(t) &= V^\dagger(t)H_0(t)V(t) - iV^\dagger(t)\frac{d}{dt}V(t) \\ &= -\sum_{k=1}^K \sum_{n=1}^K [\mathcal{G}_{kn}(t) - \mathcal{D}_{kn}(t)] |\mu_k(0)\rangle \langle \mu_n(0)| \end{aligned} \quad (4)$$

where $\mathcal{G}_{kn}(t) \equiv \langle \mu_k(t)|\dot{\mu}_n(t)\rangle$ and $\mathcal{D}_{kn}(t) \equiv \langle \mu_k(t)|H_0(t)|\mu_n(t)\rangle$ represent the geometrical and dynamical contributions to the elements of the matrix spanned by $|\mu_k(0)\rangle$, respectively.

Equation (2) can be exactly solved [63, 66] when the Hamiltonian $H_{\text{rot}}(t)$ in Eq. (4) is diagonalized, i.e., $\mathcal{G}_{kn}(t) - \mathcal{D}_{kn}(t) = 0$ for $k \neq n$. In this case, Eq. (4) can be simplified as

$$H_{\text{rot}}(t) = -\sum_{k=1}^K [\mathcal{G}_{kk}(t) - \mathcal{D}_{kk}(t)] |\mu_k(0)\rangle \langle \mu_k(0)|. \quad (5)$$

Consequently, the time-evolution operator $U_{\text{rot}}(t)$ can be directly derived from Eq. (5) as

$$U_{\text{rot}}(t) = \sum_{k=1}^K e^{if_k(t)} |\mu_k(0)\rangle \langle \mu_k(0)|, \quad (6)$$

where the global phases $f_k(t)$ ’s are defined as

$$f_k(t) \equiv \int_0^t [\mathcal{G}_{kk}(t_1) - \mathcal{D}_{kk}(t_1)] dt_1. \quad (7)$$

According to Eq. (3), the time-evolution operator $U_0(t)$ in the original picture is found to be

$$U_0(t) = V(t)U_{\text{rot}}(t) = \sum_{k=1}^K e^{if_k(t)} |\mu_k(t)\rangle \langle \mu_k(0)|. \quad (8)$$

Equation (8) implies that if the system tracks the starting point of the path $|\mu_k(0)\rangle$, it will stick to the instantaneous state $|\mu_k(t)\rangle$ and accumulate a global phase $f_k(t)$, with no transitions to the other paths $|\mu_{n \neq k}(t)\rangle$ during the time evolution.

It was proved that the diagonalization of $H_{\text{rot}}(t)$ in Eq. (5) is ensured by the von Neumann equation [51, 62]

$$\frac{d}{dt}\Pi_k(t) = -i[H_0(t), \Pi_k(t)] \quad (9)$$

with the system Hamiltonian $H_0(t)$ and the projection operator $\Pi_k(t) \equiv |\mu_k(t)\rangle\langle\mu_k(t)|$ for the ancillary state $|\mu_k(t)\rangle$. The k th path $|\mu_k(t)\rangle$ is found to be useful in universal state control except when $|\mu_k(t)\rangle$ becomes a time-independent dark state or dark mode, i.e., $|\mu_k(t)\rangle \rightarrow |\mu_k\rangle$ due to $H_0(t)|\mu_k\rangle = 0$ [67]. One can find a recipe to construct the ancillary basis states $|\mu_k(t)\rangle$'s in Ref. [67] for a general $M + N$ -dimensional system. Equation (A1) presents the results for a nondegenerate three-level system.

B. Nonideal situation

During the control dynamics, the systematic error occurs in such as the Rabi frequencies [28, 30, 33], the driving frequencies [34, 35], and the phases [27, 29, 32] of the driving fields, which is typically induced by the random fluctuation of the experimental parameters. In general, the system evolves according to

$$i \frac{d|\psi_m(t)\rangle}{dt} = H(t)|\psi_m(t)\rangle, \quad H(t) = H_0(t) + \epsilon H_1(t), \quad (10)$$

where $H_1(t)$ is the error Hamiltonian and ϵ serves as a perturbative coefficient measuring the error magnitude.

Similar to the ideal situation in Sec. II A, we start with the rotation with respect to $V(t) = \sum_{k=1}^K |\mu_k(t)\rangle\langle\mu_k(0)|$. Then the rotated Hamiltonian in Eq. (4) is rewritten as

$$H_{\text{rot}}(t) = - \sum_{k=1}^K \dot{f}_k(t) |\mu_k(0)\rangle\langle\mu_k(0)| + \epsilon \sum_{k=1}^K \sum_{n=1}^K \mathcal{D}_{kn}^{\text{err}}(t) |\mu_k(0)\rangle\langle\mu_n(0)|, \quad (11)$$

where $\mathcal{D}_{kn}^{\text{err}}(t) \equiv \langle\mu_k(t)|H_1(t)|\mu_n(t)\rangle$. The second term in Eq. (11) describes the unwanted transitions among the ancillary basis states $|\mu_k(t)\rangle$ induced by the error Hamiltonian $H_1(t)$.

To address these unwanted transitions, we consider the system dynamics in the second-rotation picture. With respect to the unitary rotation in Eq. (6), the system dynamics can be described by

$$i \frac{d|\psi_m(t)\rangle_I}{dt} = H_I(t)|\psi_m(t)\rangle_I, \quad (12)$$

where the second-rotated pure-state solution $|\psi_m(t)\rangle_I$ reads

$$|\psi_m(t)\rangle_I = U_0^\dagger(t)|\psi_m(t)\rangle_{\text{rot}}, \quad (13)$$

and the second-rotated system Hamiltonian $H_I(t)$ can be written as

$$H_I(t) = U_0^\dagger(t)H_{\text{rot}}(t)U_0(t) - iU_0^\dagger(t)\frac{d}{dt}U_0(t) = \epsilon \sum_{k=1}^K \sum_{n=1}^K \tilde{\mathcal{D}}_{kn}^{\text{err}}(t) |\mu_k(0)\rangle\langle\mu_n(0)| \equiv \epsilon \tilde{\mathcal{D}}(t), \quad (14)$$

with

$$\tilde{\mathcal{D}}_{kn}^{\text{err}}(t) \equiv \langle\mu_k(t)|H_1(t)|\mu_n(t)\rangle e^{-i[f_k(t)-f_n(t)]}. \quad (15)$$

Here $\tilde{\mathcal{D}}(t)$ is the error Hamiltonian expressed with the basis states $|\mu_k(0)\rangle$'s.

For the time-dependent Schrödinger equation (12), the time-evolution operator can be given by

$$U_I(t) = \hat{\mathcal{T}} e^{-i \int_0^t H_I(t') dt'}, \quad (16)$$

where $\hat{\mathcal{T}}$ is the time-order operator. With the Magnus expansion [68, 69] about Eq. (16), we have

$$U_I(t) = \exp \left[\sum_{l=1}^{\infty} \Lambda_l(t) \right], \quad (17)$$

where the first and second order terms are

$$\Lambda_1(t) = -i \int_0^t dt_1 H_I(t_1), \quad (18)$$

$$\Lambda_2(t) = \frac{(-i)^2}{2} \int_0^t dt_1 \int_0^{t_1} dt_2 [H_I(t_1), H_I(t_2)],$$

respectively.

Under the assumption that ϵ is both small and time-independent [27, 28], i.e., $\epsilon \ll 1$, the evolution operator in Eq. (17) can be expanded to the second order of ϵ [68]:

$$U_I(t) \approx 1 - i\epsilon \mathcal{M}(t) - \frac{\epsilon^2}{2} \left\{ \mathcal{M}(t)^2 + \int_0^t dt_1 \int_0^{t_1} dt_2 [\tilde{\mathcal{D}}(t_1), \tilde{\mathcal{D}}(t_2)] \right\}, \quad (19)$$

where $\mathcal{M}(t)$ is obtained as the time integral of the error Hamiltonian $\tilde{\mathcal{D}}(t)$

$$\mathcal{M}(t) \equiv \int_0^t dt_1 \tilde{\mathcal{D}}(t_1) \quad (20)$$

and can be regarded as an error unitary rotation.

During the evolution along the path $|\mu_k(t)\rangle$, the impact of the systematic errors can be estimated by the overlap or fidelity between the instantaneous state and the target state,

$$\mathcal{F} \equiv |\langle\mu_k(0)|U_I(t)|\mu_k(0)\rangle|^2 \approx \left| 1 - i\epsilon \mathcal{M}_{kk}(t) - \epsilon^2 \sum_{n=1}^K \int_0^t dt_1 \mathcal{M}_{nk}(t_1) \tilde{\mathcal{D}}_{kn}^{\text{err}}(t_1) \right|^2 = 1 - \epsilon^2 \sum_{n=1, n \neq k}^K |\mathcal{M}_{kn}(t)|^2 + \mathcal{O}(\epsilon^3), \quad (21)$$

where the square of the off-diagonal matrix elements $|\mathcal{M}_{kn}(t)|^2$, $k \neq n$, indicates the probability of the unwanted transitions from the desired path $|\mu_k(t)\rangle$ to other paths $|\mu_n(t)\rangle$'s. When $K = 2$, Eq. (21) recovers the results obtained by the perturbation theory in the two-level

systems [39–41]. It is straightforward to see that the error can be suppressed to the second order of ϵ when

$$\begin{aligned} & |\mathcal{M}_{kn}(t)|^2 \\ &= \left| \int_0^t \langle \mu_k(t_1) | H_1(t_1) | \mu_n(t_1) \rangle e^{-i[f_k(t_1) - f_n(t_1)]} dt_1 \right|^2 \approx 0. \end{aligned} \quad (22)$$

A brief recipe for error correction. — Equation (22) holds under at least three mechanisms: (1) The integral kernel in Eq. (22) can be divided into multiple and even infinite segments, and then the integral over each segment can be nullified, e.g., the adiabatic condition [66]. (2) The kernel itself is a periodic function [39, 41] or can be designed to be an inversely symmetrical function [69] such that the integral over the entire time domain vanishes. (3) By appropriately setting the global phases $f_k(t)$'s so that $\langle \mu_k(t) | H_1(t) | \mu_n(t) \rangle$ is a slowly-varying function with time in comparison to the exponential function $\exp[-if_k(t) + if_n(t)]$, then the overall integral approaches vanishing [44]. In other words, if we have

$$\left| \dot{f}_k(t) - \dot{f}_n(t) \right| \gg \frac{d}{dt} [\langle \mu_k(t) | H_1(t) | \mu_n(t) \rangle], \quad (23)$$

then the systematic errors can be corrected. To some extent, the correction mechanism (3) relaxes the strict requirement over the multiple vanishing segments of the integral in mechanism (1) and avoids the precise design about the periodic behavior exhibited by the integral kernel in mechanism (2).

The correction condition in Eq. (23) is mathematically supported by the Riemann-Lebesgue Lemma that if the function $\langle \mu_k(t) | H_1(t) | \mu_n(t) \rangle$ of time is Lebesgue integrable within an interval, then its Fourier coefficient such as the integral in Eq. (22) approaches vanishing with a large phase difference $|f_k(t) - f_n(t)|$. The time-evolution operator in Eq. (16) is found to be close to the identity operator in the second rotating frame under the correction condition, irrespective of the formation of $H_1(t)$, the magnitude of ϵ and even the number of nontrivial paths satisfying the von Neumann equation (9).

For a large-scale discrete-variable system, one can simply set the global phase $f_k(t)$ of the desired path $|\mu_k(t)\rangle$ as a fast-oscillating function of time and set all the other phases $f_{n \neq k}(t)$ to be constant with time. Thus the system dynamics along the nonadiabatic path $|\mu_k(t)\rangle$ can be obtained with a nearly unit fidelity, as indicated by Eqs. (21), (22), and Eq. (23). It means that at least we can have one near-perfect path and our universal error-correction strategy is scale-free. If one needs two desired paths $|\mu_{k_1}(t)\rangle$ and $|\mu_{k_2}(t)\rangle$ for a certain quantum task, then one can set $f_{k_1}(t) = -f_{k_2}(t) = f(t)$ and $f_n(t) = f_n$ for $n \neq k_1, k_2$, where $f(t)$ satisfies Eq. (23). This highlights the broad applicability of the 3rd correction mechanism. In contrast, the correction mechanism (1) or (2) is hardly practical for a high-dimensional system and is subject to various types of errors.

III. AN ILLUSTRATIVE EXAMPLE

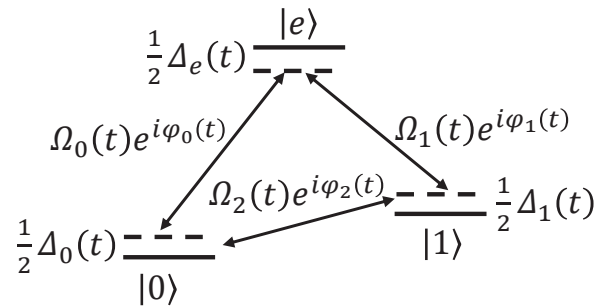


FIG. 1. Sketch of a general three-level system under control, in which the transitions $|0\rangle \leftrightarrow |e\rangle$, $|1\rangle \leftrightarrow |e\rangle$ and $|0\rangle \leftrightarrow |1\rangle$ are driven by the off-resonant driving fields.

In this section, the three-level system in Fig. 1 is used as a pedagogical example to further illustrate the correction condition in Eq. (23). The transitions among the three levels are induced by the off-resonant laser fields. In particular, the transition $|n\rangle \leftrightarrow |e\rangle$, $n = 0, 1$, is driven by the field with the time-dependent Rabi frequency $\Omega_n(t)$, phase $\varphi_n(t)$, and detuning $[\Delta_e(t) - \Delta_n(t)]/2$. The transition $|0\rangle \leftrightarrow |1\rangle$ is driven by the field $\Omega_2(t)$ with the time-dependent phase $\varphi_2(t)$ and detuning $[\Delta_1(t) - \Delta_0(t)]/2$. In experiments, the transition $|0\rangle \leftrightarrow |1\rangle$ of the superconducting transmon qubit can be achieved by a two-photon process [70]. Then the full Hamiltonian reads

$$\begin{aligned} H_0(t) &= \frac{1}{2} [\Delta_e(t)|e\rangle\langle e| + \Delta_1(t)|1\rangle\langle 1| + \Delta_0(t)|0\rangle\langle 0|] \\ &+ \left[\Omega_0(t)e^{i\varphi_0(t)}|e\rangle\langle 0| + \Omega_1(t)e^{i\varphi_1(t)}|e\rangle\langle 1| \right. \\ &\left. + \Omega_2(t)e^{i\varphi_2(t)}|1\rangle\langle 0| + \text{H.c.} \right]. \end{aligned} \quad (24)$$

To exactly solve the Schrödinger equation under the time-dependent Hamiltonian in such as Eq. (24), one can resort to the algorithm described within the ancillary picture in Sec. II A. The basis states spanning the ancillary picture [62, 67] can be chosen as

$$|\mu_1(t)\rangle = \cos \theta(t)e^{i\frac{\alpha_0(t)}{2}}|0\rangle - \sin \theta(t)e^{-i\frac{\alpha_0(t)}{2}}|1\rangle, \quad (25a)$$

$$|\mu_2(t)\rangle = \cos \phi(t)e^{i\frac{\alpha(t)}{2}}|b(t)\rangle - \sin \phi(t)e^{-i\frac{\alpha(t)}{2}}|e\rangle, \quad (25b)$$

$$|\mu_3(t)\rangle = \sin \phi(t)e^{i\frac{\alpha(t)}{2}}|b(t)\rangle + \cos \phi(t)e^{-i\frac{\alpha(t)}{2}}|e\rangle, \quad (25c)$$

where $b(t) \equiv \sin \theta(t)e^{i\alpha_0(t)/2}|0\rangle + \cos \theta(t)e^{-i\alpha_0(t)/2}|1\rangle$ is orthonormal to $|\mu_1(t)\rangle$. The undetermined parameters $\theta(t)$ and $\phi(t)$ are relevant to the population transfer, and $\alpha_0(t)$ and $\alpha(t)$ manipulate the relative phases among the states.

The ancillary basis states $|\mu_k(t)\rangle$'s could be activated as universal nonadiabatic paths when the detunings and Rabi frequencies in Hamiltonian (24) satisfy the conditions in Eqs. (A2), (A3), and (A4). Also, these non-

trivial paths construct the exact solutions to the time-dependent Schrödinger equation, i.e., the full-rank time-evolution operator in Eq. (8) with $K = 3$ or Eq. (A5), where the path-dependent global phase $f_k(t)$ can be obtained by Eq. (A6).

We take the unidirectional population transfer $|0\rangle \rightarrow |e\rangle \rightarrow |1\rangle$ along the path $|\mu_2(t)\rangle$ as an example. For this task, the time-dependent parameters $\phi(t)$ and $\theta(t)$ are required to satisfy the boundary conditions $\phi(0) = 0$, $\phi(T/2) = \pi/2$, $\phi(T) = \pi$, $\theta(0) = \pi/2$, and $\theta(T) = \pi$, where T is a characteristic period. Accordingly, one can simply set

$$\phi(t) = \frac{\pi t}{T}, \quad \theta(t) = \frac{\pi}{2} + \frac{\phi(t)}{2}, \quad (26)$$

by which the initial population on the level $|0\rangle$ can be completely transferred to the level $|e\rangle$ when $t = T/2$ and then to the level $|1\rangle$ when $t = T$. For simplicity, the global phase for the passage $|\mu_1(t)\rangle$ is assumed to be constant, i.e., $\dot{f}_1(t) = 0$. It is identified to be the parallel-transport condition for the path $|\mu_1(t)\rangle$ [47–49, 51, 59–61], which paves a way for geometric transformation under an error-free situation. Under this assumption, the global phase for the other two passages can be written as

$$\dot{f}_2(t) = \dot{f}(t), \quad \dot{f}_3(t) = -\dot{f}(t), \quad (27)$$

due to Eqs. (A6) and (A7).

Systematic error, however, emerges inevitably during the time evolution, leading to the unwanted transitions among various passages. In general, the error Hamiltonian in Eq. (10) can be classified according to whether it commutes with $H_0(t)$ or not, i.e., $[H_0(t), H_1(t)] = 0$ or $[H_0(t), H_1(t)] \neq 0$. With no loss of generality, the commutative error Hamiltonian can be written as

$$H_1(t) = \Omega_0(t)e^{i\varphi_0(t)}|e\rangle\langle 0| + \Omega_1(t)e^{i\varphi_1(t)}|e\rangle\langle 1| + \Omega_2(t)e^{i\varphi_2(t)}|1\rangle\langle 0| + \text{H.c.}, \quad (28)$$

and the noncommutative systematic error is described by

$$H_1(t) = \frac{1}{2}\Delta_1(t)|1\rangle\langle 1| + \left[\Omega_0(t)e^{i\varphi_0(t)}|e\rangle\langle 0| + \text{H.c.}\right]. \quad (29)$$

For the three-level system in the presence of the commutative error, the elements of the error rotation operator $\mathcal{M}_{kn}(t)$ in Eq. (20) are found to be

$$\begin{aligned} |\mathcal{M}_{12}(t)| &= \left| \int_0^t \frac{1}{4} \left[\dot{\alpha} + 2\dot{f} \cos(2\phi) \right] \sin(4\theta) \cos \phi e^{i(\frac{\alpha}{2} + f)} dt_1 \right|, \\ |\mathcal{M}_{13}(t)| &= \left| \int_0^t \frac{1}{4} \left[\dot{\alpha} + 2\dot{f} \cos(2\phi) \right] \sin(4\theta) \sin \phi e^{i(\frac{\alpha}{2} + f)} dt_1 \right|, \\ |\mathcal{M}_{23}(t)|^2 &= \left| \int_0^t \left\{ \dot{f} + \frac{1}{4} \left[\dot{\alpha} - 2\dot{f} \cos(2\phi) \right] \sin^2(2\theta) + i\dot{\phi} \right\} \sin(2\phi) e^{-i2f} dt_1 \right| \end{aligned} \quad (30)$$

using Eqs. (27), (28), (A8), and (A9). Here \dot{f} and $\dot{\alpha}$ are determined by Eqs. (A7) and (A9), respectively. It is found that $|\dot{\alpha}|$ will approach zero when $|\dot{f}|$ is sufficiently small.

Focusing on the kernel in the time integral, one can find that Eq. (30) provides a unified perspective to demonstrate the essences and constraints of various quantum control protocols, such as the stimulated Raman adiabatic passage [66] and the quantum holonomic transformation [51, 59]. In the stimulated Raman adiabatic passage, the Hamiltonian (24) is slowly varying with time, i.e., $\dot{\Delta}_a(t), \dot{\Omega}_a(t), \dot{\Delta}(t), \dot{\Omega}(t) \approx 0$. Suggested by Eqs. (A8) and (A9) and their time derivative, it is found that $\dot{\theta}_0(t), \dot{\alpha}_0(t), \dot{f}_1(t), \dot{\phi}(t), \dot{\alpha}(t), \dot{f}(t) \approx 0$. The off-diagonal elements $|\mathcal{M}_{kn}|$, $k \neq n \in \{1, 2, 3\}$, can then become zero under such an adiabatic control. In essence, the adiabatic control is the limiting case to the correction mechanism (1) such that the time integral is divided into infinite segments and the error can be self-corrected in each segment. The system, however, is fragile to decoherence under the greatly extended exposure to the environment and the adiabatic path is expected to fail. Under the parallel-transport condition for all the three paths in holonomic transformation [51, 59], i.e., $\dot{f}(t) = 0$, $|\mathcal{M}_{12}|$ and $|\mathcal{M}_{13}|$ in Eq. (30) will be vanishing. $|\mathcal{M}_{23}|$, however, cannot be cancelled due to the component proportional to $\dot{\phi}$. Thus it proves that the system under the holonomic transformation is significantly sensitive of to the systematic errors [60, 61]. Shortcuts to adiabaticity omitted the role of the path-dependent global phases [66] in state transfer. However, we find that they can be used as an additional degree of freedom for the robust quantum control.

In sharp contrast to the necessary condition $\dot{f}(t) = 0$ for the holonomic transformation, our error-correction condition in Eq. (23) can be reduced to a sufficiently large $|\dot{f}(t)|$ under the assumption that $\dot{f}_1 = 0$. With no loss of generality, one can simply set

$$f(t) = \lambda \phi(t), \quad (31)$$

or

$$\frac{\dot{f}}{\dot{\phi}} = \lambda, \quad (32)$$

where $\phi(t)$ can be an arbitrary smooth function of time. We hold its definition in Eq. (26) for simplicity. The coefficient λ scales the relative magnitude between $\dot{f}(t)$ and $\dot{\phi}(t)$. $\lambda = 0$ means a constant global phase or the parallel-transport condition. $\lambda \gg 1$ describes a rapid-varying global phase. With Eqs. (32), (A2), (A3), (A8), and (A9), the detunings, Rabi frequencies, and phases in the original Hamiltonian (24) can be found as

$$\begin{aligned} \Delta_e(t) &= \dot{\alpha} + 2\lambda\dot{\phi} \cos(2\phi), \\ \Delta_1(t) &= - \left[\dot{\alpha} + 2\lambda\dot{\phi} \cos(2\phi) \right] \cos^2 \theta, \\ \Delta_0(t) &= - \left[\dot{\alpha} + 2\lambda\dot{\phi} \cos(2\phi) \right] \sin^2 \theta, \end{aligned} \quad (33)$$

and

$$\begin{aligned}\Omega_0(t)e^{i\varphi_0(t)} &= -|\dot{\phi}|\sqrt{1+\lambda^2\sin^2(2\phi)}\sin\theta e^{-i\alpha_0/2}, \\ \Omega_1(t)e^{i\varphi_1(t)} &= -|\dot{\phi}|\sqrt{1+\lambda^2\sin^2(2\phi)}\cos\theta e^{i\alpha_0/2}, \\ \Omega_2(t)e^{i\varphi_2(t)} &= -\dot{\theta} - \frac{1}{4}\left[\dot{\alpha} + 2\lambda\dot{\phi}\cos(2\phi)\right]\sin(2\theta)e^{-i\alpha_0},\end{aligned}\quad (34)$$

where $\theta(t)$ and $\phi(t)$ can be arbitrarily chosen as long as their variation rates are much smaller than $|\dot{f}(t)|$. When $\lambda = 0$, Eqs. (33) and (34) are found to be consistent with the state-transfer protocol using a full-rank holonomic transformation in Ref. [62].

The power of the correction condition (32) can be analytically illustrated through the technique of integration by parts. Under the settings of $\theta(t)$, $\phi(t)$, and $f(t)$ in Eqs. (26) and (32), $\dot{\alpha}(t)$ can be estimated by Eq. (A9) as

$$\left|\frac{\dot{\alpha}(t)}{2}\right| = \left|\frac{\dot{f}\dot{\phi}^2\cos(2\phi)}{\dot{f}^2\sin^2(2\phi) + \dot{\phi}^2}\right| \leq |\dot{f}|, \quad (35)$$

where the second equality holds in case of $\phi(t) = k\pi$, $k \in Z$. Using the boundary conditions of $\theta(t)$ and $\phi(t)$ in Eq. (26), and Eqs. (32) and (35), $|\mathcal{M}_{12}(t)|$ in Eq. (30) are bounded by

$$\begin{aligned}|\mathcal{M}_{12}(T)| &\leq \left|\int_0^T F_1(t)de^{if}\right| \leq \sum_{k=0}^{\infty} \left|\int_0^T e^{if}d\left[\left(\frac{\dot{\alpha}}{2\dot{f}}\right)^k \frac{F_{\theta,\phi}}{\dot{f}}\right]\right| \\ &+ \lim_{k \rightarrow \infty} \left|\int_0^T e^{if}\left(\frac{\dot{\alpha}}{2\dot{f}}\right)^k F_1(t)dt\right|,\end{aligned}\quad (36)$$

where

$$\begin{aligned}F_1(t) &\equiv \sin(4\theta)\cos(2\phi)\cos\phi e^{i\frac{\alpha}{2}}, \\ F_{\theta,\phi} &\equiv \left[4\dot{\theta}\cos(4\theta)\cos(2\phi)\cos\phi - \dot{\phi}\sin(4\theta)\cos(2\phi)\sin\phi\right. \\ &\quad \left.- 2\dot{\phi}\sin(4\theta)\sin(2\phi)\cos\phi\right]e^{i\frac{\alpha}{2}}.\end{aligned}\quad (37)$$

It is found that the kernels of the integrals in the summation consist of an infinitesimal differential element multiplied by a periodic function when the global phase $f(t)$ is rapidly varying. Also the last term in Eq. (36) is almost zero according to Eq. (35). Consequently, $|\mathcal{M}_{12}(T)|$ vanishes within the time domain. In a similar way, the second element $|\mathcal{M}_{13}(T)|$ in Eq. (30) can be found to be vanishing in the presence of a large $|\dot{f}(t)|$.

As for the third element $|\mathcal{M}_{23}(T)|$, we have

$$|\mathcal{M}_{23}(T)| \leq \left|\int_0^T F_2(t)de^{if}\right| = \left|\int_0^T e^{if}d\left(\frac{\dot{F}_2(t)}{\dot{f}}\right)\right|, \quad (38)$$

where

$$F_2(t) = \sin(2\phi) - \sin(4\phi)\sin^2(2\theta)/4 + i\sin(2\phi)/\lambda. \quad (39)$$

It is straightforward to verify the vanishing of $|\mathcal{M}_{23}(T)|$ in the presence of a sufficiently large λ in Eq. (32).

The performance of our protocol can be evaluated by the fidelity $\mathcal{F}(T) \equiv |\langle\psi(T)|1\rangle|^2$, where $|\psi(t=T)\rangle$ is obtained by numerical simulation over the system dynamics. Practically, the wave function is obtained by the time-dependent Schrödinger equation $i\partial|\psi(t)\rangle/\partial t = [H_0(t) + \epsilon H_1(t)]|\psi(t)\rangle$ with system Hamiltonian $H_0(t)$ in Eq. (24) and error Hamiltonian $H_1(t)$ either in Eq. (28) for the commutative situation or in Eq. (29) for the noncommutative situation. While in the error-free dynamics, the system is initially prepared as $|\psi(0)\rangle = |0\rangle$ and the target states are $|\psi(T/2)\rangle = |e\rangle$ and $|\psi(T)\rangle = |1\rangle$ along the nonadiabatic paths.

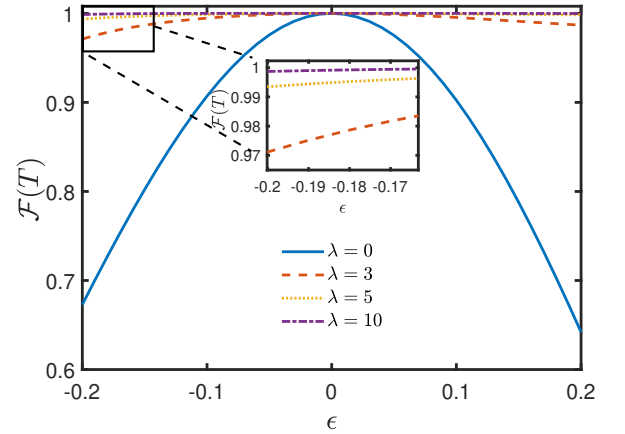


FIG. 2. Fidelity $\mathcal{F}(T)$ versus the commutative error ϵ for the complete population transfer $|0\rangle \rightarrow |e\rangle \rightarrow |1\rangle$ along the path $|\mu_2(t)\rangle$ in Eq. (25b). The detuning, the Rabi frequencies and the phases are set due to Eqs. (A2), (A3), (A8), and (A9) with $\theta(t)$ and $\phi(t)$ in Eq. (26), $f(t)$ in Eq. (32) with various coefficients λ , and $f_1(t) = \pi/2$.

In Fig. 2 with various coefficients λ , the fidelity when $t = T$ is demonstrated versus the error magnitude ϵ with the commutative error in Eq. (28). We choose $|\mu_2(t)\rangle$ in Eq. (25b) as the evolution path that could be controlled by the global phase f_2 with $|f_2(t)| = |f(t)|$. It is shown that under the conventional parallel-transport condition, i.e., $\lambda = 0$ or $\dot{f} = 0$, the fidelity is sensitive to the systematic error. In particular, $\mathcal{F} = 0.673$ when $\epsilon = -0.2$, $\mathcal{F} = 0.910$ when $\epsilon = -0.1$, $\mathcal{F} = 0.902$ when $\epsilon = 0.1$, and $\mathcal{F} = 0.642$ when $\epsilon = 0.2$. In comparison to the static global phase f , the rapidly-varying global phase $f(t)$ can efficiently correct the adverse effects arising from the commutative error. With $\lambda = \dot{f}/\dot{\phi} = 3$, the fidelity \mathcal{F} is above 0.971 in the range of $\epsilon \in [-0.2, 0.2]$. With $\lambda = 5$, the lower-bound of the fidelity is enhanced to about 0.993. And when $\lambda = 10$, the fidelity is maintained as unit even when the error magnitude is as large as 20 percentage of the original Hamiltonian.

Next we examine the validity of our error-correction mechanism in Eq. (23) in the presence of the noncommutative error in Eq. (29). It describes a type of error that

both detuning $\Delta_1(t)$ and the Rabi frequency $\Omega_0(t)$ are deviated from the original setting. In a similar way to the commutative error, using the conditions in Eqs. (27), (29), (32), (A8), and (A9) and the boundary conditions of $\theta(t)$ and $\phi(t)$, $|\mathcal{M}_{12}(t)|$ defined in Eq. (20) is found to be upper-bounded by

$$\begin{aligned} |\mathcal{M}_{12}(T)| &\leq \left| \int_0^T G_1(t) de^{if} \right|^2 + \left| \int_0^T G_2(t) de^{if} \right|^2 \\ &\leq \sum_{m=1}^2 \sum_{k=0}^{\infty} \left| \int_0^T e^{if} d \left[\left(\frac{\dot{\alpha}}{2\dot{f}} \right)^k \frac{G_{\theta,\phi}^{(m)}}{\dot{f}} \right] \right|^2 \\ &\quad + \sum_{m=1}^2 \lim_{k \rightarrow \infty} \left| \int_0^T e^{if} \left(\frac{\dot{\alpha}}{2\dot{f}} \right)^k G_m(t) dt \right|^2, \end{aligned} \quad (40)$$

where

$$\begin{aligned} G_1(t) &\equiv \sin(2\theta) \cos^2 \theta \cos(2\phi) \cos \phi e^{i\frac{\alpha}{2}}, \\ G_2(t) &\equiv \sin \theta \cos \theta \sin \phi e^{-i\frac{\alpha}{2}}, \\ G_{\theta,\phi}^{(m)} &= \dot{G}_m(t) - i\frac{\dot{\alpha}}{2} G_m(t), \quad m = 1, 2. \end{aligned} \quad (41)$$

Similar to Eqs. (36) and (38), the integrals in Eq. (40) are found to be vanishing with a large $|\dot{f}(t)|$. Similarly, the other two off-diagonal elements $|\mathcal{M}_{13}(t)|$ and $|\mathcal{M}_{23}(t)|$ in Eq. (20) are found to approach zero when λ defined in Eq. (32) is sufficiently large.

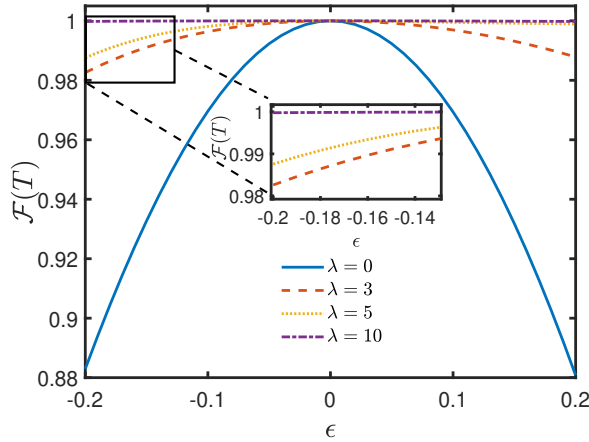


FIG. 3. Fidelity $\mathcal{F}(T)$ versus the noncommutative error ϵ for the complete population transfer $|0\rangle \rightarrow |e\rangle \rightarrow |1\rangle$ along the path $|\mu_2(t)\rangle$ in Eq. (25b). The parameters are set the same as Fig. 2, except the error Hamiltonian.

Under various coefficients λ , Fig. 3 demonstrates the fidelity when $t = T$ versus the error magnitude ϵ for the noncommutative error in Eq. (29). The chosen path $|\mu_2(t)\rangle$ embedded with our error-correction mechanism is found to be also robust against the noncommutative error, in comparison to that under the parallel-transport condition. Particularly, when the evolution satisfies $\lambda = 0$, the fidelity is about $\mathcal{F} = 0.883$ when $\epsilon = \pm 0.2$. In

contrast, the fidelity is lower-bounded by $\mathcal{F} = 0.983$ when $\lambda = 3$ and by 0.988 when $\lambda = 5$ in the range of $\epsilon \in [-0.2, 0.2]$. When $\lambda = 10$, always the fidelity remains unit irrespective of the error magnitude.

IV. CYCLIC POPULATION TRANSFER WITH ERROR CORRECTION

In this section, we intend to show the power of our error-correction protocol in the cyclic transfer of populations of the general three-level system in Fig. 1. With a distinguished error magnitude $\epsilon = -0.2$, our calculation over the state population further confirms the validity of the universal correction condition in Eq. (23) or Eq. (32).

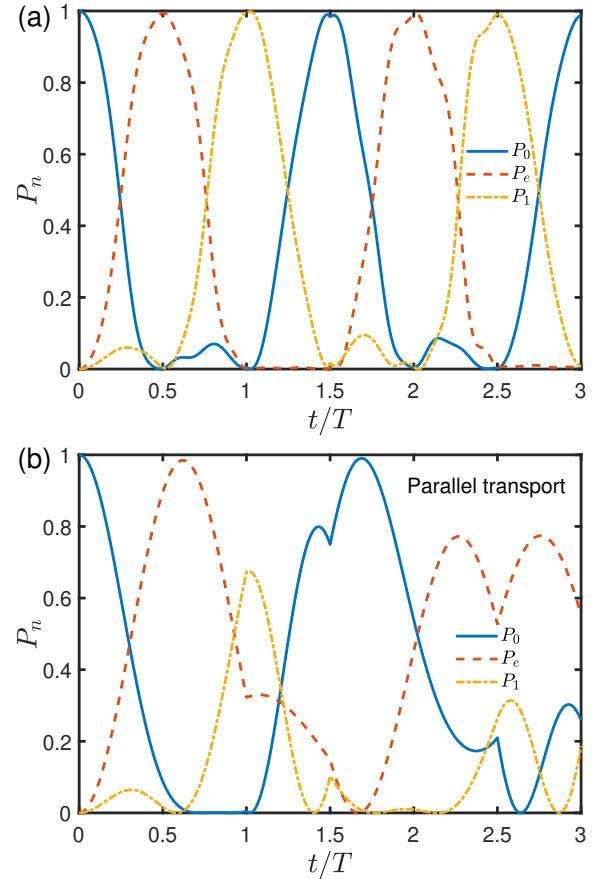


FIG. 4. State populations $P_n(t)$, $n = 0, 1, e$, under the commutative error in Eq. (28) with $\epsilon = -0.2$, versus the evolution time t/T during the cyclic population transfer. The scaling coefficient λ in Eq. (32) for the global phase $f(t)$ is fixed as (a) $\lambda = 5$ and (b) $\lambda = 0$. The detuning, the Rabi frequencies and the phases are set as Eqs. (A2), (A3), (A8) and (A9) with $\theta(t)$ and $\phi(t)$ in Eqs. (43) and (44), and $f_1(t) = \pi/2$.

A complete loop of the cyclic population transfer $|0\rangle \rightarrow |e\rangle \rightarrow |1\rangle \rightarrow |0\rangle$ can be divided into two stages, i.e., (i) $|0\rangle \rightarrow |e\rangle \rightarrow |1\rangle$ lasting T and (ii) $|1\rangle \rightarrow |0\rangle$ lasting $T/2$. On stage (i), one can employ the universal path $|\mu_2(t)\rangle$ used in the last section, in which $\theta(t)$ and $\phi(t)$ are set

according to Eq. (26). The system along the path starts from $|0\rangle$ and becomes $|e\rangle$ when $t = T/2$ and $|1\rangle$ when $t = T$. Stage (ii) employs the path $|\mu_1(t)\rangle$ in Eq. (25a), where the boundary conditions of $\theta(t)$ are $\theta(T) = \pi/2$ and $\theta(3T/2) = \pi$. Thus on stage (ii) one can simply set

$$\phi(t) = \frac{\pi t}{T}, \quad \theta(t) = \phi(t) - \frac{\pi}{2}. \quad (42)$$

Then, the population on $|1\rangle$ can be completely transferred to $|0\rangle$ when $t = 3T/2$.

In general, the k th loop of cyclic population transfer during $t \in [3(k-1)T/2, 3kT/2]$, $k \geq 1$, can be divided into two stages. On the first stage via the passage $|\mu_2(t)\rangle$, the parameters can be set as

$$\phi(t) = \frac{\pi [2t - 3(k-1)T]}{2T}, \quad \theta(t) = \frac{\pi}{2} + \frac{\phi(t)}{2}, \quad (43)$$

On the second one via $|\mu_1(t)\rangle$, we have

$$\phi(t) = \frac{\pi [2t - 3(k-1)T]}{2T}, \quad \theta(t) = \phi(t) - \frac{\pi}{2}. \quad (44)$$

When $t = 3kT/2$, the population of the system should be completely transferred back to the initial state $|0\rangle$. The presence of systematic errors, i.e., $\epsilon \neq 0$, will induce undesirable transitions among various paths during the cyclic population transfer. To demonstrate the correction effect by the global phase $f(t)$ set as Eq. (32), the performance of our protocol for the cyclic population transfer can be evaluated by the level populations $P_n(t) \equiv \langle n|\psi(t)\rangle\langle\psi(t)|n\rangle$, $n = 0, 1, e$. Note the fidelity $\mathcal{F}(T)$ defined in the last section is accurately a specified case of P_n , i.e., $\mathcal{F}(T) = P_1(t = T)$.

We compare the population dynamics P_n in the presence of the commutative error in Eq. (28) with $\epsilon = -0.2$ controlled by our protocol [see Fig. 4(a)] and the conventional parallel-transport condition [see Fig. 4(b)]. Clearly, our protocol of error correction outperforms the holonomic transformation under the parallel-transport condition. During the first loop in Fig. 4(a) with a moderate coefficient $\lambda = 5$, the initial population on the state $|0\rangle$ can be transferred to the state $|e\rangle$ with $P_e(T/2) = 0.994$. Then it can be further transferred to $|1\rangle$ with $P_1(T) = 0.994$, and back to $|0\rangle$ with $P_0(3T/2) = 0.987$. During the second loop, it is found that $P_e(2T) = 0.990$, $P_1(5T/2) = 0.991$, and $P_0(3T) = 0.989$. It means that the nearly perfect loops can be unlimitedly continued under the error correction. In sharp contrast, the cyclic population transfer under the parallel transport condition, i.e., $\lambda = 0$, is under significant impact from the systematic error as shown in Fig. 4(b). It is found $P_e(T/2) = 0.898$, $P_1(T) = 0.673$, and $P_0(3T/2) = 0.750$. Although $P_e(0.62T) = 0.984$ and $P_0(1.70T) = 0.990$ can be obtained as peak values, the cyclic population transfer can reluctantly last at most one loop with an extended period.

In the presence of noncommutative error in Eq. (29) with $\epsilon = -0.2$, the dynamics of the state populations

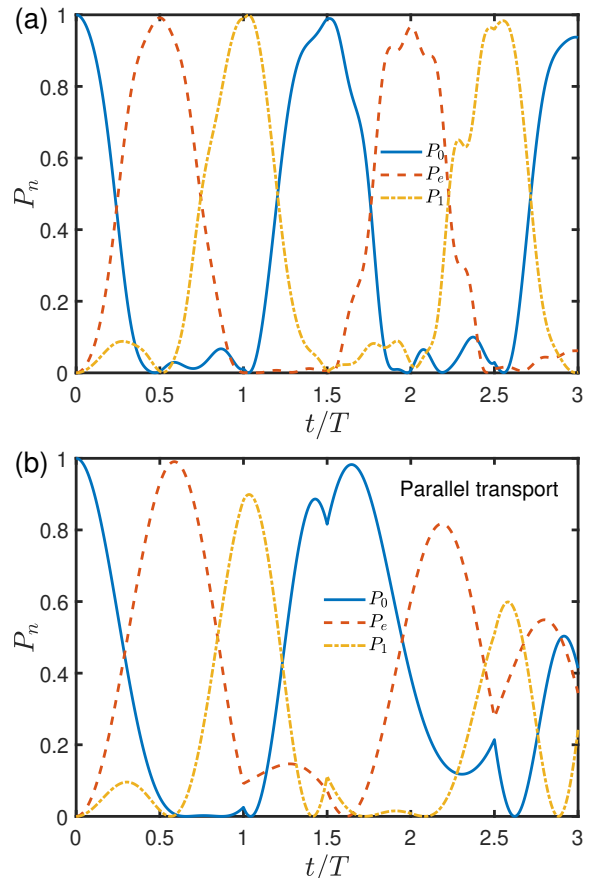


FIG. 5. State populations $P_n(t)$, $n = 0, 1, e$, under the noncommutative error in Eq. (29) with $\epsilon = -0.2$, versus the evolution time t/T during the cyclic population transfer. The global phase $f(t)$ satisfies the condition in Eq. (32) with (a) $\lambda = 5$ and (b) $\lambda = 0$. The other parameters are set the same as Fig. 4.

P_n 's are demonstrated for our protocol and that with parallel transport in Fig. 5. It is found that the adverse effects from noncommutative errors can be significantly corrected by our protocols in both populations and periods in comparison to those under the parallel-transport condition. As shown in Fig. 5(a) with $\lambda = 5$, the population is $P_e(T/2) = 0.991$, $P_1(T) = 0.990$, and $P_0(3T/2) = 0.990$ during the first loop. We still have $P_e(2T) = 0.966$, $P_1(5T/2) = 0.960$, and $P_0(3T) = 0.937$ during the second loop. In Fig. 5(b) with $\lambda = 0$, it is found that $P_e(T/2) = 0.931$, $P_1(T) = 0.890$, and $P_0(3T/2) = 0.816$. While the deviated peak values could be found as $P_e(0.60T) = 0.990$ and $P_0(1.65T) = 0.982$. The results during the second loop could not be regarded as a realistic population transfer.

V. CONCLUSION

In summary, we present a universal error-correction protocol in our forward-engineering framework for con-

control over the time-dependent discrete-variable systems within an ancillary picture, which can address arbitrary type of systematic errors. In the ideal situation, nonadiabatic paths can be generated by the von Neumann equation for the undetermined ancillary projection operators. In the presence of the systematic errors, the undesirable transitions among those paths can be corrected by the paths-dependent global phases, which have been to certain extent overlooked by conventional protocols, such as the shortcuts to adiabaticity and the holonomic quantum computation. The holonomic transformation supported by the parallel transport actually assumes a constant global phase. On the contrary, we find the rapidly-varying global phase can be used to correct both commutative and noncommutative errors. In application, we demonstrate the cyclic transfer of populations in the ubiquitous three-level system with our error correction, which could be directly extended to the systems of large scale. Our framework provides a universal error-correction theory for the quantum information processing and quantum network based on discrete-variable systems.

Appendix A: Universal paths in a three-level system

This appendix contributes to constructing universal paths, either adiabatic or nonadiabatic, for a general three-level system driven by three off-resonant driving fields, as illustrated in Fig. 1. The degree of freedom of this time-dependent system Hamiltonian is sufficiently large to yield a full-rank time-evolution operator. It can be prescribed in the ancillary rotated picture spanned by a set of completed and orthonormal basis states. According to the brief recipe in Refs. [62, 67], the ancillary basis states can be written as

$$\begin{aligned} |\mu_1(t)\rangle &= \cos\theta(t)e^{i\frac{\alpha_0(t)}{2}}|0\rangle - \sin\theta(t)e^{-i\frac{\alpha_0(t)}{2}}|1\rangle, \\ |\mu_2(t)\rangle &= \cos\phi(t)e^{i\frac{\alpha(t)}{2}}|b(t)\rangle - \sin\phi(t)e^{-i\frac{\alpha(t)}{2}}|e\rangle, \\ |\mu_3(t)\rangle &= \sin\phi(t)e^{i\frac{\alpha(t)}{2}}|b(t)\rangle + \cos\phi(t)e^{-i\frac{\alpha(t)}{2}}|e\rangle, \end{aligned} \quad (\text{A1})$$

where $b(t) \equiv \sin\theta(t)e^{i\alpha_0(t)/2}|0\rangle + \cos\theta(t)e^{-i\alpha_0(t)/2}|1\rangle$ is orthonormal to $|\mu_1(t)\rangle$. $\theta(t)$, $\alpha_0(t)$, $\phi(t)$, and $\alpha(t)$ are the time-dependent parameters to be determined. These states apply to any three-level systems and could be easily extended to larger-size systems.

Substituting the ancillary basis states in Eq. (A1) into the von Neumann equation (9) with the Hamiltonian in Eq. (24), the detunings and the Rabi-frequencies in the lab frame are found to be

$$\begin{aligned} \Delta_e(t) &= \Delta(t), \\ \Delta_1(t) &= -\Delta(t)\cos^2\theta(t) + \Delta_a(t), \\ \Delta_0(t) &= -\Delta(t)\sin^2\theta(t) - \Delta_a(t), \end{aligned} \quad (\text{A2})$$

and

$$\begin{aligned} \Omega_0(t)e^{i\varphi_0(t)} &= \Omega(t)\sin\theta(t)e^{-i\frac{\alpha_0(t)}{2}}, \\ \Omega_1(t)e^{i\varphi_1(t)} &= \Omega(t)\cos\theta(t)e^{i\frac{\alpha_0(t)}{2}}, \\ \Omega_2(t)e^{i\varphi_2(t)} &= \Omega_a(t) - \frac{1}{2}\Delta(t)\sin\theta(t)\cos\theta(t)e^{-i\alpha_0(t)}, \end{aligned} \quad (\text{A3})$$

respectively, where the scaling detunings $\Delta(t)$ and $\Delta_a(t)$ and the scaling Rabi frequencies $\Omega(t)$ and $\Omega_a(t)$ satisfy the following conditions

$$\begin{aligned} \Delta_a(t) &= \dot{\alpha}_0(t) + 2\Omega_a(t)\cot 2\theta(t)\cos\alpha_0(t), \\ \Omega_a(t) &= -\frac{\dot{\theta}(t)}{\sin\alpha_0(t)}, \\ \Delta(t) &= \dot{\alpha}(t) + 2\Omega(t)\cot 2\phi(t)\cos\alpha(t) + \Omega_a(t)\frac{\cos\alpha_0(t)}{\sin 2\theta(t)}, \\ \Omega(t) &= -\frac{\dot{\phi}(t)}{\sin\alpha(t)}. \end{aligned} \quad (\text{A4})$$

According to Eq. (8), the time-evolution operator for the three-level system (24) can be written as

$$U(t, 0) = \sum_{k=1}^3 e^{if_k(t)}|\mu_k(t)\rangle\langle\mu_k(0)|, \quad (\text{A5})$$

where the global phases can be expressed as

$$\begin{aligned} \dot{f}_1(t) &= \Omega_a(t)\frac{\cos\alpha_0(t)}{\sin 2\theta(t)} = -\dot{\theta}(t)\frac{\cot\alpha_0(t)}{\sin 2\theta(t)}, \\ \dot{f}_2(t) &= \dot{f}(t) - \frac{1}{2}\dot{f}_1(t), \\ \dot{f}_3(t) &= -\dot{f}(t) - \frac{1}{2}\dot{f}_1(t) \end{aligned} \quad (\text{A6})$$

with

$$\dot{f}(t) = \Omega(t)\frac{\cos\alpha(t)}{\sin 2\phi(t)} = -\dot{\phi}(t)\frac{\cot\alpha(t)}{\sin 2\phi(t)}. \quad (\text{A7})$$

With no loss of generality, one can choose $\theta(t)$, $\phi(t)$, $f_1(t)$, and $f(t)$ as independent variables in practical control. Then under the conditions in Eqs. (A6) and (A7), Eq. (A4) can be rewritten as

$$\begin{aligned} \Delta_a(t) &= \dot{\alpha}_0(t) + 2\dot{f}_1(t)\cos 2\theta(t), \\ \Omega_a(t) &= -\sqrt{\dot{\theta}(t)^2 + \dot{f}_1(t)^2\sin^2 2\theta(t)}, \\ \dot{\alpha}_0(t) &= -\frac{\dot{\theta}\dot{f}_1\sin 2\theta - \dot{f}_1\dot{\theta}\sin 2\theta - 2\dot{f}_1\dot{\theta}^2\cos 2\theta}{\dot{f}_1^2\sin^2 2\theta + \dot{\theta}^2}, \end{aligned} \quad (\text{A8})$$

and

$$\begin{aligned} \Delta(t) &= \dot{\alpha}(t) + 2\dot{f}(t)\cos 2\phi(t) + \dot{f}_1(t), \\ \Omega(t) &= -\sqrt{\dot{\phi}(t)^2 + \dot{f}(t)^2\sin^2 2\phi(t)}, \\ \dot{\alpha}(t) &= -\frac{\dot{\phi}\dot{f}\sin 2\phi - \dot{f}\dot{\phi}\sin 2\phi - 2\dot{f}\dot{\phi}^2\cos 2\phi}{\dot{f}^2\sin^2 2\phi + \dot{\phi}^2}. \end{aligned} \quad (\text{A9})$$

It is found that the system evolution along the path $|\mu_1(t)\rangle$ is determined by the parameters $\theta(t)$ and $f_1(t)$ or $f(t)$, which can be controlled by $\Delta_a(t)$ and $\Omega_a(t)$ in Eq. (A8). Similarly, the setting of $\phi(t)$ and $f_1(t)$ or $f(t)$ determines the evolution along the path $|\mu_2(t)\rangle$ or $|\mu_3(t)\rangle$, which is controlled by $\Delta(t)$ and $\Omega(t)$ in Eq. (A9). Equation (A9) shares the similar form as Eq. (A8), due to the fact that the transition between the states $|b(t)\rangle$ and $|e\rangle$ is equivalent to that in an effective two-level system.

In regard of the first derivative of Eqs. (A8) and (A9) with respect to time, one can find that a slowly-varying Hamiltonian in Eq. (24) with $\dot{\Delta}_a(t), \dot{\Omega}_a(t), \dot{\Delta}(t), \dot{\Omega}(t) \approx 0$ yields the vanishing of the first and second derivatives of the parameters with respect to time, including $\theta_0(t)$, $\alpha_0(t)$, $f_1(t)$, $\phi(t)$, $\alpha(t)$, and $f(t)$. Consequently, the elements $\mathcal{M}_{kn}(t)$ in Eq. (30) can become zero under the stimulated Raman adiabatic passage.

-
- [1] J. Preskill, *Quantum computing in the nisq era and beyond*, **Quantum** **2**, 79 (2018).
- [2] S. Bravyi, D. Gosset, and R. König, *Quantum advantage with shallow circuits*, **Science** **362**, 308 (2018).
- [3] A. Ekert and R. Jozsa, *Quantum computation and shor's factoring algorithm*, **Rev. Mod. Phys.** **68**, 733 (1996).
- [4] I. Kivlichan, C. Gidney, D. Berry, N. Wiebe, J. McClean, W. Sun, Z. Jiang, N. Rubin, A. Fowler, A. Aspuru-Guzik, H. Neven, and R. Babbush, *Improved fault-tolerant quantum simulation of condensed-phase correlated electrons via trotterization*, **Quantum** **4**, 1 (2020).
- [5] C. Gidney and M. Ekerå, *How to factor 2048 bit rsa integers in 8 hours using 20 million noisy qubits*, **Quantum** **5**, 433 (2019).
- [6] J. P. Gaebler, T. R. Tan, Y. Lin, Y. Wan, R. Bowler, A. C. Keith, S. Glancy, K. Coakley, E. Knill, D. Leibfried, and D. J. Wineland, *High-fidelity universal gate set for $^9\text{Be}^+$ ion qubits*, **Phys. Rev. Lett.** **117**, 060505 (2016).
- [7] M. A. Rol, F. Battistel, F. K. Malinowski, C. C. Bultink, B. M. Tarasinski, R. Vollmer, N. Haider, N. Muthusubramanian, A. Bruno, B. M. Terhal, and L. DiCarlo, *Fast, high-fidelity conditional-phase gate exploiting leakage interference in weakly anharmonic superconducting qubits*, **Phys. Rev. Lett.** **123**, 120502 (2019).
- [8] B. Foxen, C. Neill, A. Dunsworth, P. Roushan, B. Chiaro, A. Megrant, J. Kelly, Z. Chen, K. Satzinger, R. Barends, F. Arute, K. Arya, R. Babbush, D. Bacon, J. C. Bardin, S. Boixo, D. Buell, B. Burkett, Y. Chen, R. Collins, E. Farhi, A. Fowler, C. Gidney, M. Giustina, R. Graff, M. Harrigan, T. Huang, S. V. Isakov, E. Jeffrey, Z. Jiang, D. Kafri, K. Kechedzhi, P. Klimov, A. Korotkov, F. Kostritsa, D. Landhuis, E. Lucero, J. McClean, M. McEwen, X. Mi, M. Mohseni, J. Y. Mutus, O. Naaman, M. Neeley, M. Niu, A. Petukhov, C. Quintana, N. Rubin, D. Sank, V. Smelyanskiy, A. Vainsencher, T. C. White, Z. Yao, P. Yeh, A. Zalcman, H. Neven, and J. M. Martinis (Google AI Quantum), *Demonstrating a continuous set of two-qubit gates for near-term quantum algorithms*, **Phys. Rev. Lett.** **125**, 120504 (2020).
- [9] Y. Wu, W.-S. Bao, S. Cao, F. Chen, M.-C. Chen, X. Chen, T.-H. Chung, H. Deng, Y. Du, D. Fan, M. Gong, C. Guo, C. Guo, S. Guo, L. Han, L. Hong, H.-L. Huang, Y.-H. Huo, L. Li, N. Li, S. Li, Y. Li, F. Liang, C. Lin, J. Lin, H. Qian, D. Qiao, H. Rong, H. Su, L. Sun, L. Wang, S. Wang, D. Wu, Y. Xu, K. Yan, W. Yang, Y. Yang, Y. Ye, J. Yin, C. Ying, J. Yu, C. Zha, C. Zhang, H. Zhang, K. Zhang, Y. Zhang, H. Zhao, Y. Zhao, L. Zhou, Q. Zhu, C.-Y. Lu, C.-Z. Peng, X. Zhu, and J.-W. Pan, *Strong quantum computational advantage using a superconducting quantum processor*, **Phys. Rev. Lett.** **127**, 180501 (2021).
- [10] P. W. Shor, *Scheme for reducing decoherence in quantum computer memory*, **Phys. Rev. A** **52**, R2493 (1995).
- [11] M. A. Nielsen and I. L. Chuang, *Quantum Computation and Quantum Information: 10th Anniversary Edition* (Cambridge University Press, 2010).
- [12] L. Egan, D. M. Debroy, C. Noel, A. Risinger, D. Zhu, D. Biswas, M. Newman, M. Li, K. R. Brown, M. Cetina, and C. Monroe, *Fault-tolerant control of an error-corrected qubit*, **Nature** **598**, 281 (2021).
- [13] C. Ryan-Anderson, J. G. Bohnet, K. Lee, D. Gresh, A. Hankin, J. P. Gaebler, D. Francois, A. Chernoguzov, D. Lucchetti, N. C. Brown, T. M. Gatterman, S. K. Halit, K. Gilmore, J. A. Gerber, B. Neyenhuis, D. Hayes, and R. P. Stutz, *Realization of real-time fault-tolerant quantum error correction*, **Phys. Rev. X** **11**, 041058 (2021).
- [14] M. H. Abobeih, Y. Wang, J. Randall, S. J. H. Loenen, C. E. Bradley, M. Markham, D. J. Twitchen, B. M. Terhal, and T. H. Taminiou, *Fault-tolerant operation of a logical qubit in a diamond quantum processor*, **Nature** **606**, 884 (2021).
- [15] N. Sundaresan, T. J. Yoder, Y. Kim, M. Li, E. H. Chen, G. Harper, T. Thorbeck, A. W. Cross, A. D. Córcoles, and M. Takita, *Demonstrating multi-round subsystem quantum error correction using matching and maximum likelihood decoders*, **Nat. Commun.** **14**, 2852 (2023).
- [16] S. Krinner, N. Lacroix, A. Remm, A. Di Paolo, E. Genois, C. Leroux, C. Hellings, S. Lazar, F. Swiadek, J. Herrmann, G. J. Norris, C. K. Andersen, M. Müller, A. Blais, C. Eichler, and A. Wallraff, *Realizing repeated quantum error correction in a distance-three surface code*, **Nature** **605**, 669 (2022).
- [17] Y. Zhao, Y. Ye, H.-L. Huang, Y. Zhang, D. Wu, H. Guan, Q. Zhu, Z. Wei, T. He, S. Cao, F. Chen, T.-H. Chung, H. Deng, D. Fan, M. Gong, C. Guo, S. Guo, L. Han, N. Li, S. Li, Y. Li, F. Liang, J. Lin, H. Qian, H. Rong, H. Su, L. Sun, S. Wang, Y. Wu, Y. Xu, C. Ying, J. Yu, C. Zha, K. Zhang, Y.-H. Huo, C.-Y. Lu, C.-Z. Peng, X. Zhu, and J.-W. Pan, *Realization of an error-correcting surface code with superconducting qubits*, **Phys. Rev. Lett.** **129**, 030501 (2022).
- [18] N. Ofek, A. Petrenko, R. Heeres, P. Reinhold, Z. Leghtas, B. Vlastakis, Y. Liu, L. Frunzio, S. M. Girvin, L. Jiang, M. Mirrahimi, M. H. Devoret, and R. J. Schoelkopf, *Extending the lifetime of a quantum bit with error correction in superconducting circuits*, **Nature** **536**, 441 (2016).
- [19] C. Flühmann, T. L. Nguyen, M. Marinelli, V. Negnevitsky, K. Mehta, and J. P. Home, *Encoding a qubit in a trapped-ion mechanical oscillator*, **Nature** **566**, 513 (2019).

- [20] P. Campagne-Ibarcq, A. Eickbusch, S. Touzard, E. Zalts-Geller, N. E. Frattini, V. V. Sivak, P. Reinhold, S. Puri, S. Shankar, R. J. Schoelkopf, L. Frunzio, M. Mirrahimi, and M. H. Devoret, *Quantum error correction of a qubit encoded in grid states of an oscillator*, *Nature* **584**, 368 (2020).
- [21] A. Grimm, N. E. Frattini, S. Puri, S. O. Mundhada, S. Touzard, M. Mirrahimi, S. M. Girvin, S. Shankar, and M. H. Devoret, *Stabilization and operation of a kerr-cat qubit*, *Nature* **584**, 205 (2020).
- [22] G. Q. AI, *Suppressing quantum errors by scaling a surface code logical qubit*, *Nature* **614**, 676 (2023).
- [23] Z. Ni, S. Li, X. Deng, Y. Cai, L. Zhang, W. Wang, Z.-B. Yang, H. Yu, F. Yan, S. Liu, C.-L. Zou, L. Sun, S.-B. Zheng, Y. Xu, and D. Yu, *Beating the break-even point with a discrete-variable-encoded logical qubit*, *Nature* **616**, 56 (2022).
- [24] A. Paetznick, M. P. da Silva, C. Ryan-Anderson, J. M. Bello-Rivas, J. P. C. III, A. Chernoguzov, J. M. Dreiling, C. Foltz, F. Frachon, J. P. Gaebler, T. M. Gatterman, L. Grans-Samuellsson, D. Gresh, D. Hayes, N. Hewitt, C. Holliman, C. V. Horst, J. Johansen, D. Lucchetti, Y. Matsuoka, M. Mills, S. A. Moses, B. Neyenhuis, A. Paz, J. Pino, P. Siegfried, A. Sundaram, D. Tom, S. J. Wernli, M. Zanner, R. P. Stutz, and K. M. Svore, *Demonstration of logical qubits and repeated error correction with better-than-physical error rates*, *arXiv: 2404.02280* (2024).
- [25] M. H. Levitt, *Composite pulses*, *Prog. Nucl. Magn. Reson. Spectrosc.* **18**, 61 (1986).
- [26] R. Tycko, *Broadband population inversion*, *Phys. Rev. Lett.* **51**, 775 (1983).
- [27] N. V. Vitanov, *Arbitrarily accurate narrowband composite pulse sequences*, *Phys. Rev. A* **84**, 065404 (2011).
- [28] X. Wang, L. S. Bishop, J. Kestner, E. Barnes, K. Sun, and S. Das Sarma, *Composite pulses for robust universal control of singlet-triplet qubits*, *Nat. Commun.* **3**, 997 (2012).
- [29] E. Kyoseva and N. V. Vitanov, *Arbitrarily accurate pass-band composite pulses for dynamical suppression of amplitude noise*, *Phys. Rev. A* **88**, 063410 (2013).
- [30] J. P. Kestner, X. Wang, L. S. Bishop, E. Barnes, and S. Das Sarma, *Noise-resistant control for a spin qubit array*, *Phys. Rev. Lett.* **110**, 140502 (2013).
- [31] X. Wang, L. S. Bishop, E. Barnes, J. P. Kestner, and S. D. Sarma, *Robust quantum gates for singlet-triplet spin qubits using composite pulses*, *Phys. Rev. A* **89**, 022310 (2014).
- [32] G. T. Genov, D. Schraft, T. Halfmann, and N. V. Vitanov, *Correction of arbitrary field errors in population inversion of quantum systems by universal composite pulses*, *Phys. Rev. Lett.* **113**, 043001 (2014).
- [33] X.-C. Yang, M.-H. Yung, and X. Wang, *Neural-network-designed pulse sequences for robust control of singlet-triplet qubits*, *Phys. Rev. A* **97**, 042324 (2018).
- [34] B. T. Torosov and N. V. Vitanov, *Robust high-fidelity coherent control of two-state systems by detuning pulses*, *Phys. Rev. A* **99**, 013424 (2019).
- [35] E. Kyoseva, H. Greener, and H. Suchowski, *Detuning-modulated composite pulses for high-fidelity robust quantum control*, *Phys. Rev. A* **100**, 032333 (2019).
- [36] Z.-C. Shi, H.-N. Wu, L.-T. Shen, J. Song, Y. Xia, X. X. Yi, and S.-B. Zheng, *Robust single-qubit gates by composite pulses in three-level systems*, *Phys. Rev. A* **103**, 052612 (2021).
- [37] H.-N. Wu, C. Zhang, J. Song, Y. Xia, and Z.-C. Shi, *Composite pulses for optimal robust control in two-level systems*, *Phys. Rev. A* **107**, 023103 (2023).
- [38] A. Ruschhaupt, X. Chen, D. Alonso, and J. G. Muga, *Optimally robust shortcuts to population inversion in two-level quantum systems*, *New J. Phys.* **14**, 093040 (2012).
- [39] D. Daems, A. Ruschhaupt, D. Sugny, and S. Guérin, *Robust quantum control by a single-shot shaped pulse*, *Phys. Rev. Lett.* **111**, 050404 (2013).
- [40] Y. Liang, Y.-X. Wu, and Z.-Y. Xue, *Nonadiabatic geometric quantum gates that are robust against systematic errors*, *Phys. Rev. Appl.* **22**, 024061 (2024).
- [41] G. Dridi, K. Liu, and S. Guérin, *Optimal robust quantum control by inverse geometric optimization*, *Phys. Rev. Lett.* **125**, 250403 (2020).
- [42] G. Dridi, X. Laforgue, M. Mejatty, and S. Guérin, *Optimal ultrarobust quantum gates by inverse optimization*, *Phys. Rev. A* **109**, 062613 (2024).
- [43] T. Propson, B. E. Jackson, J. Koch, Z. Manchester, and D. I. Schuster, *Robust quantum optimal control with trajectory optimization*, *Phys. Rev. Appl.* **17**, 014036 (2022).
- [44] J. Jing, L.-A. Wu, M. Byrd, J. Q. You, T. Yu, and Z.-M. Wang, *Nonperturbative leakage elimination operators and control of a three-level system*, *Phys. Rev. Lett.* **114**, 190502 (2015).
- [45] M. Harutyunyan, F. Holweck, D. Sugny, and S. Guérin, *Digital optimal robust control*, *Phys. Rev. Lett.* **131**, 200801 (2023).
- [46] F. Zhang, J. Zhang, P. Gao, and G. Long, *Searching nonadiabatic holonomic quantum gates via an optimization algorithm*, *Phys. Rev. A* **100**, 012329 (2019).
- [47] M.-Z. Ai, S. Li, R. He, Z.-Y. Xue, J.-M. Cui, Y.-F. Huang, C.-F. Li, and G.-C. Guo, *Experimental realization of nonadiabatic holonomic single-qubit quantum gates with two dark paths in a trapped ion*, *Fundam. Res.* **2**, 661 (2022).
- [48] T. André and E. Sjöqvist, *Dark path holonomic qudit computation*, *Phys. Rev. A* **106**, 062402 (2022).
- [49] Z.-y. Jin and J. Jing, *Geometric quantum gates via dark paths in rydberg atoms*, *Phys. Rev. A* **109**, 012619 (2024).
- [50] P. Z. Zhao and J. Gong, *Mitigation of systematic amplitude error in nonadiabatic holonomic operations*, *Phys. Rev. A* **110**, 012426 (2024).
- [51] B.-J. Liu, X.-K. Song, Z.-Y. Xue, X. Wang, and M.-H. Yung, *Plug-and-play approach to nonadiabatic geometric quantum gates*, *Phys. Rev. Lett.* **123**, 100501 (2019).
- [52] G. T. Genov, B. T. Torosov, and N. V. Vitanov, *Optimized control of multistate quantum systems by composite pulse sequences*, *Phys. Rev. A* **84**, 063413 (2011).
- [53] X. Chen, E. Torrontegui, and J. G. Muga, *Lewis-riesenfeld invariants and transitionless quantum driving*, *Phys. Rev. A* **83**, 062116 (2011).
- [54] D. Guéry-Odelin, A. Ruschhaupt, A. Kiely, E. Torrontegui, S. Martínez-Garaot, and J. G. Muga, *Shortcuts to adiabaticity: Concepts, methods, and applications*, *Rev. Mod. Phys.* **91**, 045001 (2019).
- [55] S.-f. Qi and J. Jing, *Accelerated adiabatic passage in cavity magnomechanics*, *Phys. Rev. A* **105**, 053710 (2022).
- [56] X. Chen, I. Lizuain, A. Ruschhaupt, D. Guéry-Odelin, and J. G. Muga, *Shortcut to adiabatic passage in two-*

- three-level atoms*, *Phys. Rev. Lett.* **105**, 123003 (2010).
- [57] J. Jing, M. S. Sarandy, D. A. Lidar, D.-W. Luo, and L.-A. Wu, *Eigenstate tracking in open quantum systems*, *Phys. Rev. A* **94**, 042131 (2016).
- [58] A. Baksic, H. Ribeiro, and A. A. Clerk, *Speeding up adiabatic quantum state transfer by using dressed states*, *Phys. Rev. Lett.* **116**, 230503 (2016).
- [59] E. Sjöqvist, D. M. Tong, L. M. Andersson, B. Hessmo, M. Johansson, and K. Singh, *Non-adiabatic holonomic quantum computation*, *New J. Phys.* **14**, 103035 (2012).
- [60] J. Jing, C.-H. Lam, and L.-A. Wu, *Non-abelian holonomic transformation in the presence of classical noise*, *Phys. Rev. A* **95**, 012334 (2017).
- [61] S.-B. Zheng, C.-P. Yang, and F. Nori, *Comparison of the sensitivity to systematic errors between nonadiabatic non-abelian geometric gates and their dynamical counterparts*, *Phys. Rev. A* **93**, 032313 (2016).
- [62] Z.-y. Jin and J. Jing, *Universal perspective on nonadiabatic quantum control*, *Phys. Rev. A* **111**, 012406 (2025).
- [63] M. V. Berry, *Transitionless quantum driving*, *J. Phys. A* **42**, 365303 (2009).
- [64] N. V. Golubev and A. I. Kuleff, *Control of populations of two-level systems by a single resonant laser pulse*, *Phys. Rev. A* **90**, 035401 (2014).
- [65] S. González-Resines, D. Guéry-Odelin, A. Tobalina, I. Lizuain, E. Torrontegui, and J. G. Muga, *Invariant-based inverse engineering of crane control parameters*, *Phys. Rev. Appl.* **8**, 054008 (2017).
- [66] N. V. Vitanov, A. A. Rangelov, B. W. Shore, and K. Bergmann, *Stimulated raman adiabatic passage in physics, chemistry, and beyond*, *Rev. Mod. Phys.* **89**, 015006 (2017).
- [67] Z.-y. Jin and J. Jing, *Entangling distant systems via universal nonadiabatic passage*, *Phys. Rev. A* **111**, 022628 (2025).
- [68] S. Blanes, F. Casas, J. Oteo, and J. Ros, *The magnus expansion and some of its applications*, *Phys. Rep.* **470**, 151 (2009).
- [69] B.-J. Liu, Y.-S. Wang, and M.-H. Yung, *Superrobust nonadiabatic geometric quantum control*, *Phys. Rev. Res.* **3**, L032066 (2021).
- [70] A. Vepsäläinen, S. Danilin, and G. S. Paraoanu, *Supera-
diabatic population transfer in a three-level superconducting circuit*, *Sci. Adv.* **5**, eaau5999 (2019).